

SIMULATION OF FATIGUE CRACK PROPAGATION IN THE WING MAIN SPAR FLANGE

Petr Augustin¹

¹ Institute of Aerospace Engineering
Brno University of Technology
Technická 2, 616 69 Brno, Czech Republic
augustin@fme.vutbr.cz

Keywords: fatigue crack growth, wing spar, fatigue test, BEM, SHM

Abstract: Simulation of fatigue crack growth in the bottom flange of twin turboprop commuter aircraft wing spar is described in this paper. Analysed crack propagation scenario represents real wing full-scale fatigue test failure. Computational model of bottom flange was prepared using three-dimensional fracture mechanics software FRANC3D. Calculation of crack growth under the variable amplitude loading was performed in AFGROW code using the NASGRO equation and Wheeler retardation model. It was verified with the results of wing spar specimen fatigue test and fractographic analysis of fatigue fracture from this experiment. Computational model was applied in the prognostic algorithm of structure health monitoring system.

NOMENCLATURE

a	crack length
da/dN	crack growth rate
G	shear modulus
K	stress intensity factor
K_c	fracture toughness
K_{op}	opening stress intensity factor
ΔK_{th}	threshold stress intensity factor range
R	stress ratio
α	constraint factor
ν	Poisson's ratio
σ_o	flow stress
σ_{ys}	tensile yield strength

1 INTRODUCTION

The paper deals with the simulation of fatigue crack growth in the bottom flange of twin turboprop commuter aircraft wing spar. The main goal was to develop the crack propagation model applicable in the prognostic algorithm of structure health monitoring (SHM) system based on ultrasonic method [1]. The work was carried out within the frame of ENTIS project - Evaluation of SHM methods and its integration into aircraft maintenance system supported by Czech Ministry of Industry and Trade (project description can be found in the Appendix).

Crack in the main wing spar flange near the rib No. 8 initiated during the full-scale fatigue test of the wing at Aeronautical Research and Test Institute in Prague [2] was selected for the analysis. In this particular wing box design, major portion of the bending loads is carried by the main spar and crack arrest capability of stiffeners is negligible. Identical crack growth scenario was also simulated during the fatigue test of the flange specimens performed in the ENTIS project. Results of fractographic analysis of flange fracture from this test were used for verification of crack propagation simulation.

2 BEM MODEL OF THE WING SPAR FLANGE

Computational model of cracked bottom flange was prepared using the software FRANC3D developed at the Cornell University [3]. FRANC3D is pre and postprocessor specialized on fracture mechanics problems. It is efficient tool for simulation of arbitrary cracks in the components of aircraft structures [4-6] or engines [7]. FRANC3D is capable to write the input files among others for the BEM (Boundary Element Method) code BES that was used for the analysis of the flange.

The BEM model of the flange (Figure 1) represents the cross section of the flange in the location of real approximately planar fatigue crack emanating from the rivet hole of the flange - skin connection. It is expected that the initial flaw is in the form of two opposite corner cracks with the radius of 1.27 mm (Figure 2). The BEM model was in one end fixed and in the second loaded via the surface boundary condition defining linear distribution of stress along the height of the flange cross section. Numerical values of stresses were derived from dynamical strain gauge measurements performed during the fatigue test of the wing structure [2]. Stress redistribution between the cracked spar and the skin stripes was modelled using local loading introduced in the rivet positions. Rivet forces were obtained from FEM model (MSC.Patran/Nastran) of cracked flange - skin connection (Figure 5) with the rivet joints represented using BUSH elements having the flexibility determined according to Swift [8]. 42 BEM models containing 60 crack fronts have been prepared and solved by the BES code (Figures 2-4). They represent two different phases of propagation of cracks in the flange. The first one is propagation of two cracks initiated in the opposite corners of the rivet hole and this phase is finished by unstable propagation of outer crack. The second phase represents subsequent propagation of single inner crack heading toward the centre of the spar, again terminated by crack instability resulting in the final failure of the flange.

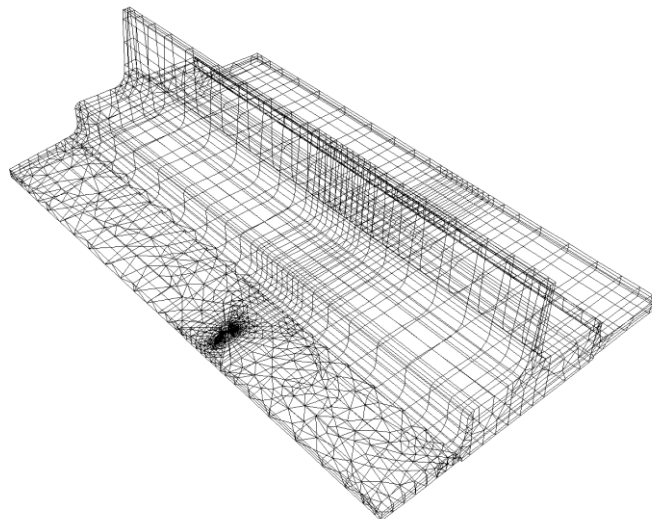


Figure 1: BEM model of the flange

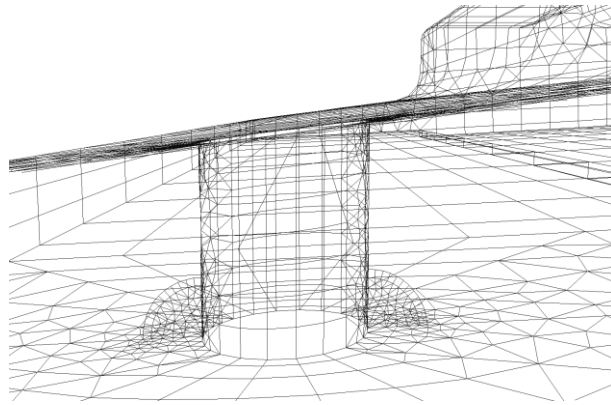


Figure 2: Detail of the BEM model - initial corner cracks with the radius of 1.27 mm (crack fronts 0)

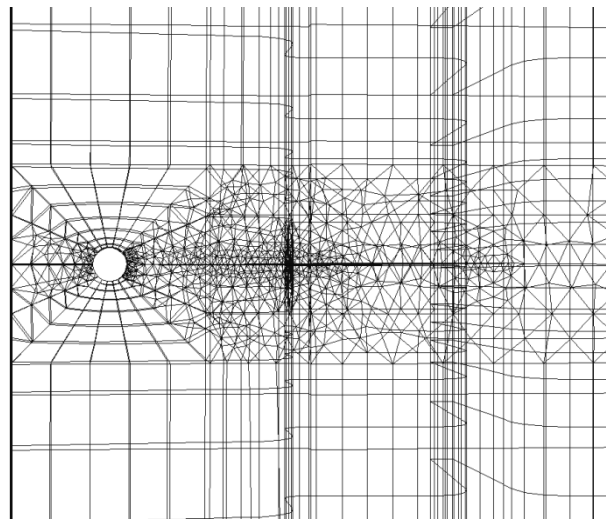


Figure 3: Detail of the BEM mesh (crack front 40)

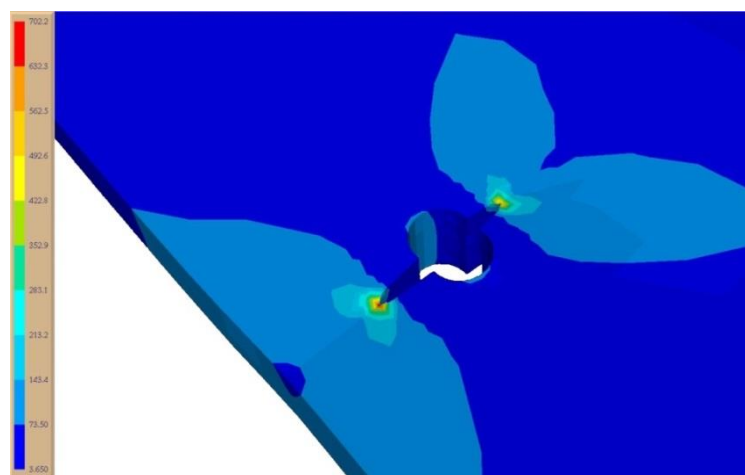


Figure 4: Von Mises stress field around the crack in FRANC3D (crack fronts 14)

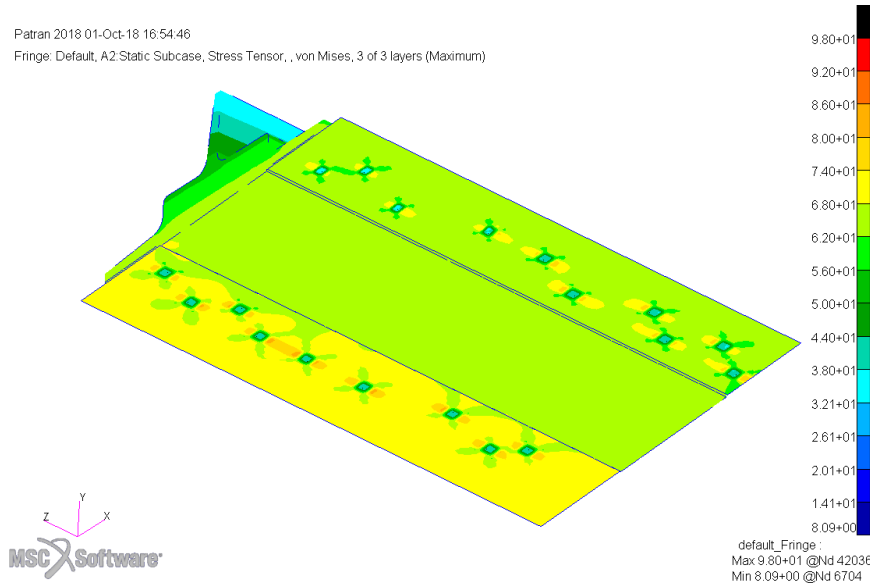


Figure 5: Von Mises stress contour plot in Patran indicating position of flange-skin connection rivets

FRANC3D calculates stress intensity factors using the displacement correlation technique [3, 9]:

$$K_I = \frac{G}{\kappa + 1} \sqrt{\frac{2\pi}{L_Q}} [4(v_B - v_D) - (v_C - v_E)] \quad (1)$$

$$K_{II} = \frac{G}{\kappa + 1} \sqrt{\frac{2\pi}{L_Q}} [4(u_B - u_D) - (u_C - u_E)] \quad (2)$$

where κ is $(3 - \nu)/(1 + \nu)$ for plane stress, $3 - 4\nu$ for plane strain and L_Q is the length of an element along the crack face (see Figure 6). Figure 7 shows opening mode I K-factor values along selected crack fronts, Figure 8 then summarizes K_I values obtained along the flange bottom surface. The sliding II and tearing III mode stress intensity factors were more or less close to zero during the simulation depending on the maximum crack growth increment selected for the calculation of next crack fronts. The increments along the crack front less than selected maximum were determined using the formula:

$$\Delta l = \Delta l_{max} \frac{K_I^n}{K_{I,max}^n} \quad (3)$$

where n is exponent of the crack growth law applied.

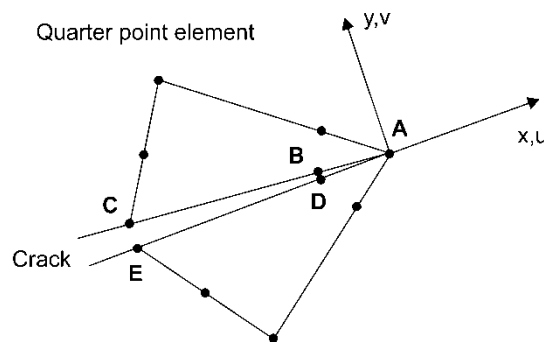


Figure 6: Nomenclature for stress intensity factor computation [9]

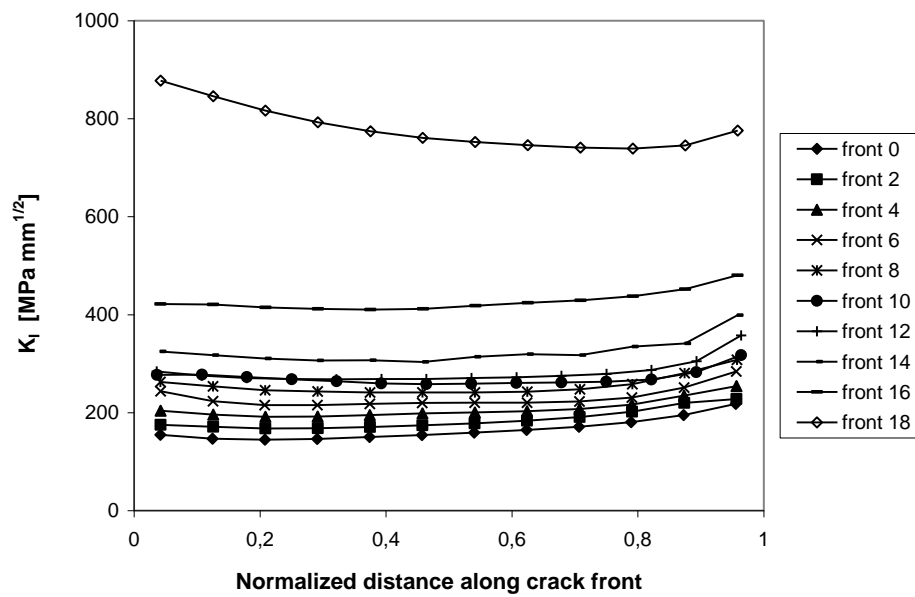


Figure 7: Mode I stress intensity factor along selected outer crack fronts

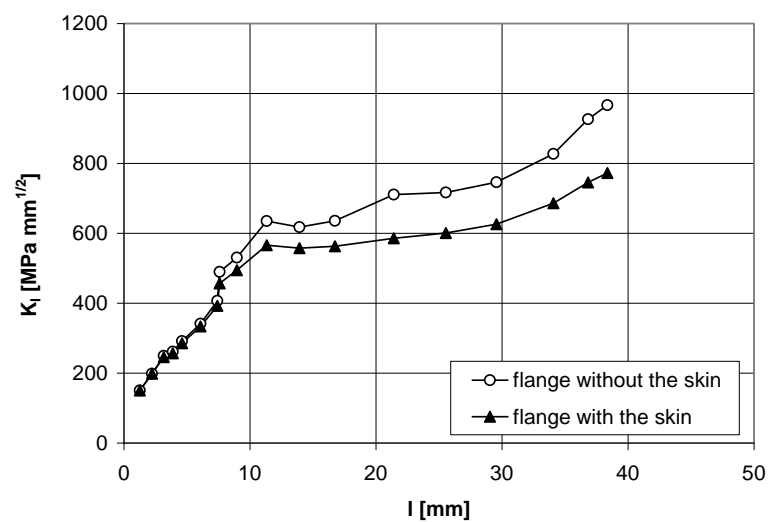


Figure 8: Mode I stress intensity factor for inner crack along the flange bottom surface

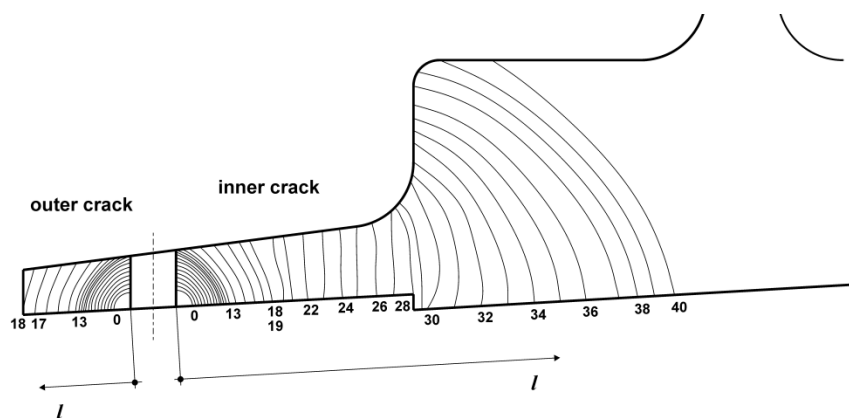


Figure 9: Overview of calculated crack fronts

3 CRACK GROWTH MODEL

Calculation of crack propagation was carried out in AFGROW software [10]. Applied crack growth rate relationship called NASGRO equation [11] is given by:

$$\frac{da}{dN} = C \left[\left(\frac{1-f}{1-R} \right) \Delta K \right]^n \frac{\left(1 - \frac{\Delta K_{th}}{\Delta K} \right)^p}{\left(1 - \frac{K_{max}}{K_C} \right)^q} \quad (4)$$

where crack opening function is defined as:

$$f = \frac{K_{op}}{K_{max}} = \begin{cases} \max(R, A_0 + A_1 R + A_2 R^2 + A_3 R^3), & R \geq 0 \\ A_0 + A_1 R, & -2 \leq R < 0 \end{cases} \quad (5)$$

The coefficients are expressed as:

$$\begin{aligned} A_0 &= (0.825 - 0.34 \alpha + 0.05 \alpha^2) \left[\cos \left(\frac{\pi}{2} \frac{\sigma_{max}}{\sigma_0} \right) \right]^{\frac{1}{\alpha}} \\ A_1 &= (0.415 - 0.071 \alpha) \frac{\sigma_{max}}{\sigma_0} \\ A_2 &= 1 - A_0 - A_1 - A_3 \\ A_3 &= 2A_0 + A_1 - 1 \end{aligned} \quad (6)$$

Application of NASGRO 4.23 data set for 2024-T3511 aluminium alloy extrusion leads to the dependency of crack growth rate on the stress intensity factor range shown in Figure 10.

The program block from the full-scale fatigue test of the wing was applied in the simulation. One program block consists of 199 basic program cycles followed by one extended program cycle. Basic program cycle representing one flight contains 6 constant amplitude (CA) cycles of ground loads followed by 9 CA cycles of vertical gusts on two load levels and 6 CA horizontal gust cycles. Extended program cycle contains also one extra 7.5 m/s vertical gust cycle. Moreover marking program cycles enabling fractographic reconstitution based on the identification of beach marks on the fracture surface were also applied in the intervals adopted from the verification spar flange fatigue test (Figure 11).

Interaction of overload and subsequent smaller cycles in the loading sequence reduce the rate of crack growth. Retardation effect was handled through the Wheeler model [12]. Crack growth rate calculated by the equation (4) is modified by the retardation factor C_p :

$$\left(\frac{da}{dN} \right)_r = C_p \frac{da}{dN} \quad (7)$$

where:

$$C_p = \left(\frac{r_p}{a_{OL} + (r_p)_{OL} - a} \right)^m \quad (8)$$

Retardation factor is given by the crack and plastic zone sizes for overload (OL) cycle and subsequent smaller cycles and by the empirical constant m . Plastic zone size was calculated by the equation:

$$r_p = \frac{1}{k\pi} \left(\frac{K_{max}}{\sigma_{YS}} \right)^2 \quad (9)$$

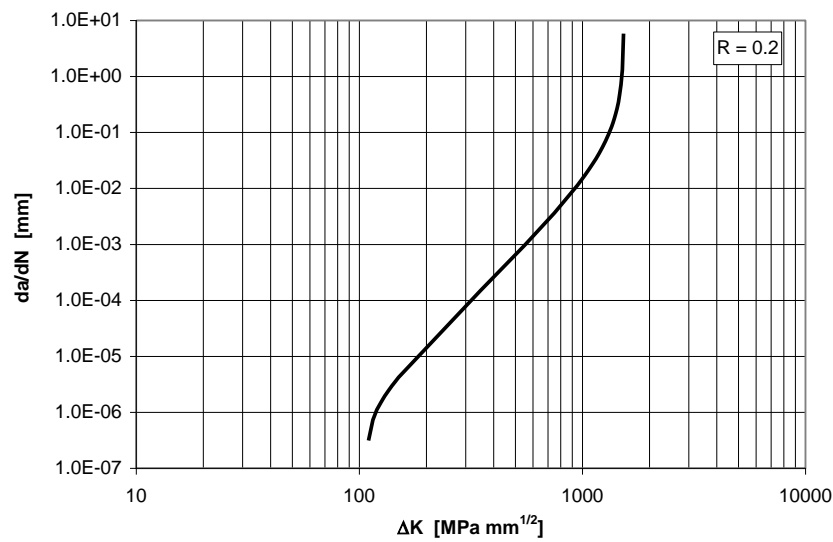


Figure 10: Crack growth rate of 2024-T3511 aluminium alloy extrusion

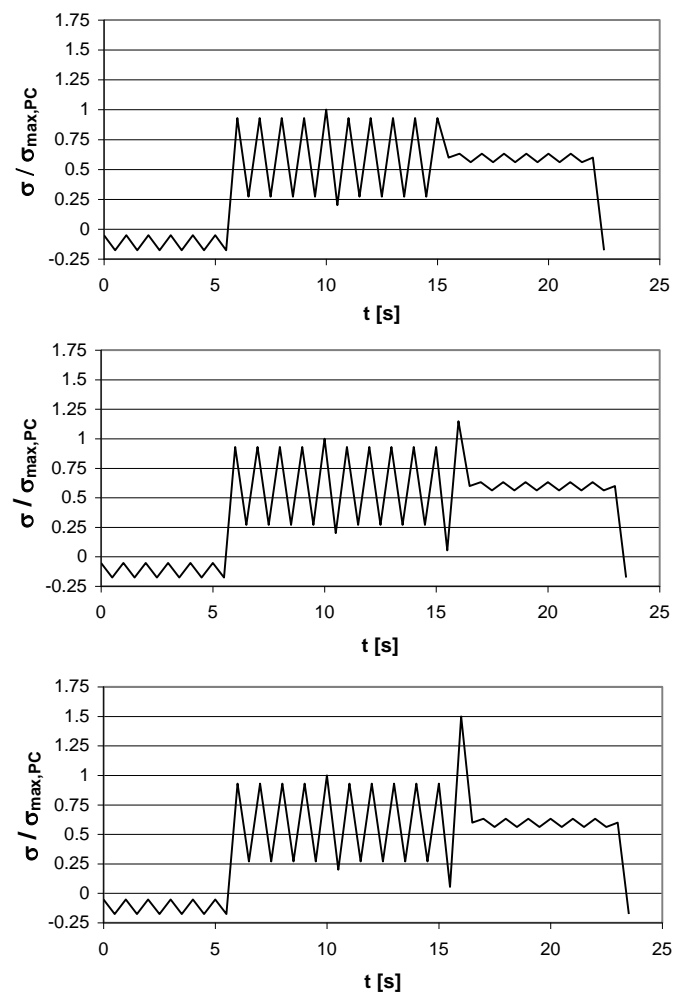


Figure 11: Stress in the bottom flange during the basic, extended and marking program cycle

where $k = 2$ for plane stress and $k = 6$ for plane strain. Intermediate values were determined by empirical equation [10]:

$$k = 6.7037 - \frac{1.4972}{t} \left(\frac{K_{max}}{\sigma_{YS}} \right)^2 \quad (10)$$

where t is part thickness.

4 SIMULATION RESULTS AND VERIFICATION FATIGUE TEST

Crack propagation curves obtained from the simulations using both the non-interaction and Wheeler models are depicted in Figure 12. Wheeler retardation model was correlated with the experimental data obtained from verification fatigue test of the wing spar flange specimen (Figure 13).

The test was carried out using 200 kN servohydraulic loading frame in two phases. In the first one, the clean flange was tested under the constant amplitude loading in order to create initial corner cracks in the hole on the notches manufactured by electric discharge machine. The notches were subsequently removed by drilling to a higher diameter, the hole was filled by the rivet and the specimen was completed by manufacturing of the spar-skin joint. In the second phase carried out under the variable amplitude loading described in previous paragraph, propagation of fatigue cracks in the flange was optically monitored by travelling microscopes. Marking program cycles were applied according to anticipated or observed crack propagation rate. Fractographic analysis of the flange fracture surface from this test was performed at the Department of Materials, Faculty of Nuclear Sciences and Physical Engineering, Czech Technical University in Prague [13]. Beach marks created by the marking program cycles were identified on the fracture surface and used for verification of simulation as shown in Figure 12.

Crack growth scenario in Figure 12 is based on an assumption of symmetrical initiation of two corner cracks in the rivet hole. Application in the prognostic algorithm for prediction of remaining crack growth life for crack lengths measured by SHM system however requires generalization of the model to unsymmetrical scenarios. This problem was solved by additional analyses in FRAN3D and corresponding modifications of computational model.

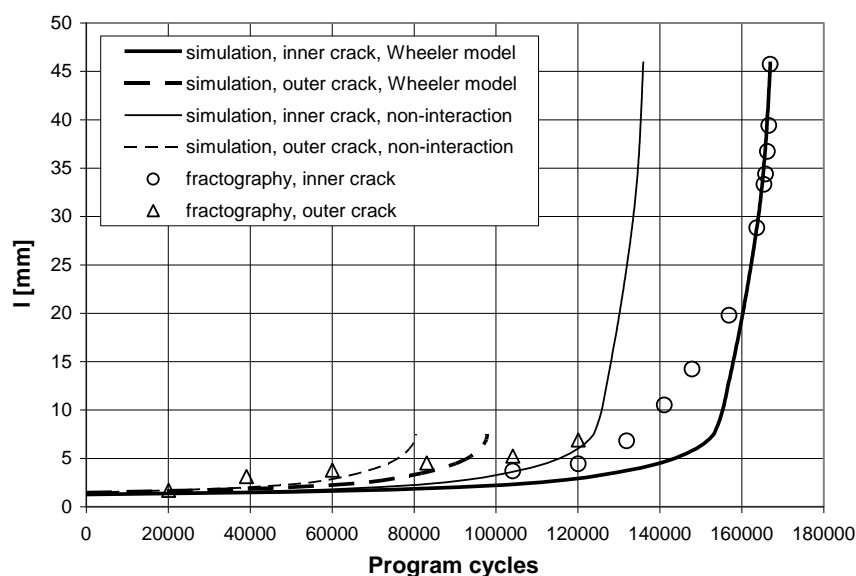


Figure 12: Crack propagation curves at the flange bottom surface obtained using the simulation and by the fractographic reconstitution

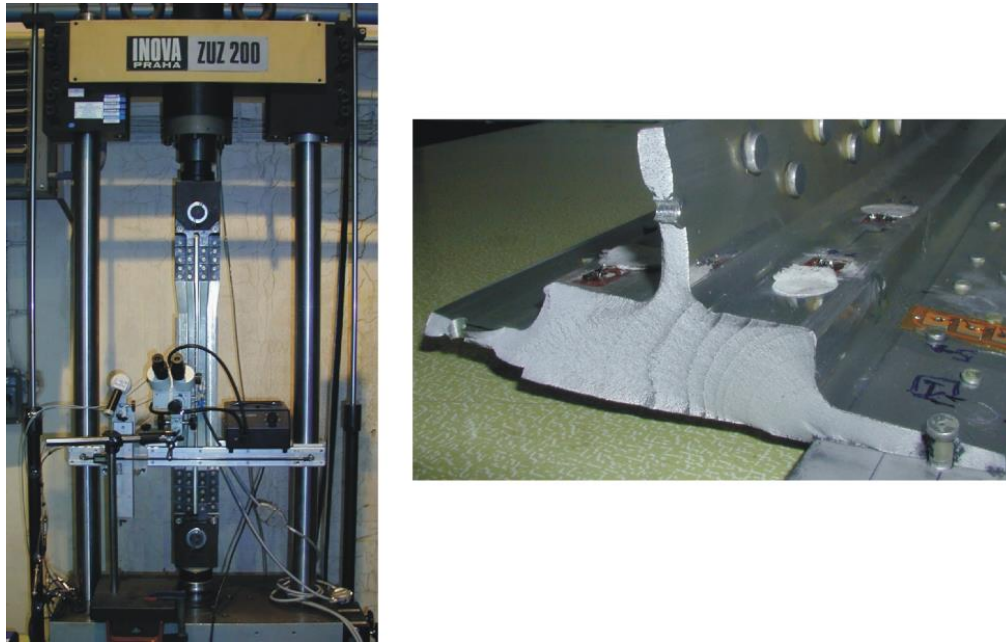


Figure 13: Fatigue test of the spar flange specimen and flange fracture surface

5 CONCLUSION

Simulation of fatigue crack propagation in the bottom flange of twin turboprop commuter aircraft wing spar was carried out. It utilizes the BEM model of spar flange prepared in the three-dimensional crack propagation software FRANC3D to calculate the crack fronts and stress intensity factors. Analysed crack propagation scenario represents real wing full-scale fatigue test failure. Prediction of crack growth under the variable amplitude loading is based on the NASGRO equation and Wheeler retardation model. It was verified with the results of wing spar specimen fatigue test and fractographic analysis of fatigue fracture from this experiment. Computational model was applied in the prognostic algorithm of structure health monitoring system.

REFERENCES

- [1] Finda, J.; Vechart, A.; Hédli, R. (2012). Prediction of fatigue crack growth in airframe structures. In: *First European Conference of the Prognostics and Health Management Society*.
- [2] Běhal, J. (2010). Proposal of the loading sequence for tests of the wing spar flange specimen. Tech. rep. ADATO.0508.V.U.TR, Aeronautical Research and Test Institute Prague (in Czech).
- [3] FRANC3D, Concepts & users guide, Version 2.6. Cornell Fracture Group.
- [4] Miedlar, P. C.; Berens, A. P.; Gunderson, A.; Gallagher, J. P. (2002). Analysis and support initiative for structural technology (ASIST) - USAF damage tolerant design handbook: Guidelines for the analysis and design of damage tolerant aircraft structures. Tech. rep. AFRL-VA-WP-TR-2003-3002, Air Vehicles Directorate, WPAFB, OH.
- [5] Hassiotis, S.; Gould, S. C. (2004). Fracture analysis of the F-5, 15%-spar bolt. *Engineering Failure Analysis*, 11, 355-360.
- [6] Materna, A. (1999). Modelling of propagation of planar fatigue cracks in 3D. Ph.D. thesis, Department of Materials, Faculty of Nuclear Sciences and Physical Engineering, Czech Technical University in Prague (in Czech).

- [7] Barlow, K., W.; Chandra, R. (2005). Fatigue crack propagation simulation in an aircraft engine fan blade attachment. *International Journal of Fatigue* 27, 1661–1668.
- [8] Swift, T. (1984). Fracture analysis of stiffened structure. In: *Damage Tolerance of Metallic Structures: Analysis Methods and Application*. ASTM STP 842.
- [9] Lim, I. L.; Johnston, I. W.; Choi, S. K. (1992). Comparison between various displacement-based stress intensity factor computation techniques. *International Journal of Fracture* 58, 193–210.
- [10] Harter, J. A. (2008). AFGROW Users guide and technical manual. Air Vehicles Directorate, WPAFB, OH.
- [11] NASGRO reference manual. NASA Johnson Space Center, Southwest Research Institute.
- [12] Farahmand, B.; Bockrath, G.; Glassco, J. (1997). *Fatigue and Fracture Mechanics of High Risk Parts, Application of LEFM & FMDM Theory*. Chapman & Hall.
- [13] Kovářík, O.; Siegl, J. (2012). Fractographic analysis of aircraft main spar fractures. Tech. rep. V-KMAT-846/12, Department of Materials, Faculty of Nuclear Sciences and Physical Engineering, Czech Technical University in Prague (in Czech).

APPENDIX

The aim of the **ENTIS project** (full title Evaluation of SHM methods and its integration into aircraft maintenance system) was research and development of a new technology for monitoring of fatigue and corrosion damage of airframe structure critical parts. The partners in the project consortium were Honeywell International, Aircraft Industries, Brno University of Technology, Academy of Sciences of the Czech Republic and SVÚOM Ltd.. Permanently attached ultrasonic and acoustic emission sensors were implemented for continuous or periodical signal data collection on the aircraft parts monitored during the fatigue and corrosion laboratory tests. Besides others, several fatigue tests of complex specimens representing fatigue critical components of commuter aircraft airframe have been done. Objective of the tests was benchmark of the sensors and signal database collection. Development of the analytics for the monitored structure damage prediction under given operational conditions was also an important part of the ENTIS project.

COPYRIGHT STATEMENT

The authors confirm that they, and/or their company or organization, hold copyright on all of the original material included in this paper. The authors also confirm that they have obtained permission, from the copyright holder of any third party material included in this paper, to publish it as part of their paper. The authors confirm that they give permission, or have obtained permission from the copyright holder of this paper, for the publication and distribution of this paper as part of the READ 2018 proceedings.

This is an open access article distributed under the [Creative Commons Attribution License](https://creativecommons.org/licenses/by/4.0/) which permits unrestricted use, distribution, and reproduction in any medium, provided the original work is properly cited. (CC BY 4.0).